Contents lists available at ScienceDirect

Applied Catalysis B: Environmental

Hydrated electron (e$_{aq}^-$) generation from p-benzoquinone/UV: Combined experimental and theoretical study

Jia Gu[a], Ling Yang[b], Jun Ma[a,*], Jin Jiang[a,*], Jingxin Yang[c], Jianqiao Zhang[a], Huizhong Chi[a], Yang Song[a], Shaofang Sun[a], Wei Quan Tian[d]

[a] State Key Laboratory of Urban Water Resource and Environment, School of Municipal and Environmental Engineering, Harbin Institute of Technology, Harbin, Heilongjiang 150090, PR China
[b] MIIT Key Laboratory of Critical Materials Technology for New Energy Conversion and Storage, School of Chemistry and Chemical Engineering, Harbin Institute of Technology, Harbin, Heilongjiang 150080, PR China
[c] School of Chemical Engineering and Technology, Sun Yat-sen University, Zhuhai 519082, PR China
[d] College of Chemistry and Chemical Engineering, Chongqing University, Chongqing 401331, PR China

ARTICLE INFO

ABSTRACT

A p-benzoquinone (p-BQ)/UV process to induce hydrated electron (e$_{aq}^-$) generation was predicted by quantum chemical calculations and validated by experiment in this work. Theoretically, the photolysis of p-BQ under UV irradiation at 253.7 nm could induce water to generate e$_{aq}^-$ with a molar ratio of 1:2 via the direct triplet mechanism, in which 1,4-addition reaction of the first triplet state of p-BQ with water was the key step. Experimentally, monochloroacetic acid (MCAA) (the probe of e$_{aq}^-$) was used to detect e$_{aq}^-$ generated in the p-BQ/UV process. The generation efficiency showed a positive linear dependence on the p-BQ concentration, which illustrated the crucial role of p-BQ on the generation of e$_{aq}^-$. During the photolysis, p-hydroquinone was the primary intermediate for the generation of e$_{aq}^-$. Kinetically, the energy barriers of the e$_{aq}^-$ generation from p-HOC$_6$H$_4$OH, p-HOC$_6$H$_4$O$^-$ and p-$^-$OC$_6$H$_4$O$^-$ were 100.8 kcal mol^{-1}, 46.5 kcal mol^{-1} and 5.6 kcal mol^{-1}, respectively. Both the experimental and theoretical results show that the generation of e$_{aq}^-$ was much more efficient from the anions than that from p-HOC$_6$H$_4$OH. The findings in the present study may help to understand the mechanism of e$_{aq}^-$ generation from natural organic matters (NOM), since quinone-like groups are usually contained in NOM.

© 2017 Elsevier B.V. All rights reserved.

1. Introduction

Recently, advanced reduction processes (ARPs) [1] have drawn attention for the remediation of contaminated environments [2–6], especially for the decontamination of chlorinated [2–5] and fluorinated organic pollutants [7–11]. As one of the most reductive species, hydrated electron (e$_{aq}^-$) (with the standard reduction potential of about −2.9 V) [12] is the optimal one for ARPs. The structure of e$_{aq}^-$ can be simplified as an excess electron stabilized by a known number of oriented water molecules [13–15]. The behavior of e$_{aq}^-$ is just like an anion, and the size of the anion is similar to that of the iodide ion [12]. Through a one-electron transfer process [2,8,12], e$_{aq}^-$ can react with many substrates, which have more positive standard reduction potentials, with consid-

erable rate constants [12]. The rate constants vary with a range from 10^1 L mol^{-1} s^{-1} up to the diffusion controlled limit [12]. The activation energies for the reactions are from 1.4 kcal mol^{-1} to 7.2 kcal mol^{-1} [12], which are invariably small and moderate.

In the reactions with organic molecules, the reactivity of e$_{aq}^-$ is determined by the structures of the reacting molecules, and a great enhancement is induced by the electron-withdrawing substituents [12]. As electron-withdrawing substituents, the substituent halogen atoms can be eliminated as the halide ion (X$^-$) by e$_{aq}^-$ [12], which is the theoretical foundation of the decontamination of chlorinated and fluorinated organic pollutants by ARPs with e$_{aq}^-$ as reductant [2–5,7–11]. Since the reductive degradation of persistent pollutants by the concurrent electron acceptance [16,17] usually transforms the organic pollutants into more environmentally benign and biodegradable products [1,16], it is obvious that the e$_{aq}^-$ based ARPs are important and promising for the pollution remediation. Usually, e$_{aq}^-$ can be generated from some common inorganic reducing agents, e.g., sulfite [1–7], ferrous iron [18], and iodide [8,9,11,19]. However, there have been few studies about

the generation of e_{aq}^- involving quinones (common organic compounds) [20].

Quinones are a group of highly reactive organic compounds [20], which are abundant in the environment [20]. Quinones can act as electron-shuttle, being the important active center in some chemical and biochemical processes [21–23]. Actually, the reactivity of quinone is determined by its redox cycling, where the reduction of quinone to semiquinone anion radical or hydroquinone is reversible [24]. In addition, it has been well demonstrated that the formation of p-hydroquinone can be induced by the photoreactions of p-BQ (an oxidation intermediate of phenol [25]) in aqueous solution under UV irradiation at 253.7 nm [26], in which the redox cycling is involved [26]. With the formation of p-hydroquinone, it is reasonable to expect the generation of e_{aq}^- by the UV photolysis of p-BQ in aqueous solution [27]. Joschek et al. have studied the generation of e_{aq}^- from p-hydroquinone without oxygen in the solution under steady irradiation at 253.7 nm, and they found that p-hydroquinone could generate e_{aq}^- and p-BQ, with semiquinone radical as the intermediate [27]. Nevertheless, further investigations should be conducted to examine the dependence of the e_{aq}^- generation upon pH. In addition, the mechanism of the formation of p-hydroquinone by the UV photolysis of p-BQ in aqueous solution is still a matter of debate, which warrants further studies.

Several studies have reported some distinct mechanisms of the UV photolysis of p-BQ in aqueous solution, which can lead to the formation of similar products, namely the hydroquinone and hydroxylated quinone [26,30–33]. These mechanisms are classified as the OH$^\bullet$ [30–32], direct triplet [26], and quinone-quinone or electron transfer mechanisms [26,33]. These mechanisms are initiated by the same steps: the excitation of quinone to its first excited singlet state, followed by the intersystem crossing to its first triplet state [26,28–33]. In the OH$^\bullet$ mechanism, the abstraction of hydrogen atom from water molecule by the first triplet state of quinone can induce the formation of OH$^\bullet$ radical and semiquinone radical, and the two radicals can lead to the formation of the hydroquinone and hydroxylated quinone [30–32]. In the direct triplet mechanism, the first triplet state of quinone reacts with water molecule directly, leading to the formation of benzene-1,2,4-triol with rearrangement, and then benzene-1,2,4-triol can be oxidized by quinone, resulting in the formation of the hydroquinone and hydroxylated quinone with a molar ratio of 1:1 [26]. At high concentrations of quinone, the first triplet state of quinone may oxidize quinone by one electron transfer, leading to the formation of semiquinone radical anion and cation, which is designated as the electron transfer mechanism [26,33]. Then, the hydroquinone and hydroxylated quinone can be generated from the semiquinone radical anion and cation [26,33].

Recently, we have reported that the UV photolysis of phenol at 253.7 nm in aqueous solution could induce the generation of e_{aq}^- with a molar ratio of 1:4 via two periods [34]. In the phenol/UV process, we have theoretically confirmed that p-hydroquinone was much more readily to be generated from the hydrogen abstraction of the adduct by phenoxyl radical (rather than from the photolysis of the phenoxyl radical dimers), which makes it possible to generate four moles of e_{aq}^- from one mole of phenol with p-benzoquinone as the product [34]. With the recycling of phenoxyl radical, one mole of phenol could release two moles of e_{aq}^- with p-hydroquinone as the product in period I [34]. The generation of e_{aq}^- could also be induced by the UV photolysis of p-hydroquinone with p-BQ as the product [27], which was the period II [34]. Since the UV photolysis of p-BQ in aqueous solution has the potential for the generation of e_{aq}^-, it is necessary to investigate the transformation of p-BQ in the similar system [34], which can help to improve the understanding of the e_{aq}^- generation in the phenol/UV process [34].

In this work, the theoretical confirmation of the mechanism of the formation of p-hydroquinone in the p-BQ/UV process was

performed by the quantum chemical calculations, and the energy barrier of the generation of e_{aq}^- from p-hydroquinone was also calculated. Then, the crucial role of p-BQ on the generation of e_{aq}^- was experimentally explored. Further, the role of the e_{aq}^- probe in the process was confirmed, and the correlation between the amounts of p-BQ and the e_{aq}^- probe degraded was studied to illuminate the stoichiometric ratio for the e_{aq}^- generation. Finally, the dependence of the e_{aq}^- generation upon pH was experimentally investigated, which was interpreted with the assistance of the calculated energy barrier of the generation of e_{aq}^- from p-hydroquinone. Based on the investigation above, the influence of the addition of phenol on the e_{aq}^- generation in the p-BQ/UV process was also examined. Monochloroacetic acid (MCAA) was used as the probe of e_{aq}^- (1.0×10^9 M^{-1} s^{-1}) [12], and the e_{aq}^- generation efficiency was determined by the degradation of MCAA.

2. Experimental

2.1. Materials and reagents

Without further purification, all chemicals from commercial source were dissolved in ultra-pure water (18.2 MΩ cm), which was generated by a Milli-Q Biocel water system. Phenol (ACS reagent, ≥99.0%), p-BQ (reagent grade, ≥98%), sodium monochloroacetate (98%), acetic acid (ACS reagent, ≥99.7%), potassium hydroxide (sigmaultra, ≥85%), sodium chloride (99.999%), sodium hydroxide (ACS reagent, ≥97.0%), sodium tetraborate decahydrate (ACS reagent, ≥99.5%), sodium phosphate dibasic (ACS reagent, ≥99.0%), sodium phosphate monobasic monohydrate (ACS reagent, 98.0 ∼ 102.0%), potassium iodide (ACS reagent, ≥99.0%) and potassium iodate (ACS reagent, 99.5%) were supplied by Sigma-Aldrich. Methanol (HPLC Grade) was purchased from Fisher Chemical. Hydrogen peroxide (H_2O_2, 35% v/v, stab.) was obtained from Alfa Aesar.

2.2. Experimental procedure

Photolysis experiments were conducted in a sealed cylindrical borosilicate glass reactor ($V = 1000$ mL), equipped with a 15 W low-pressure mercury UV lamp (253.7 nm, ozone-free, GPH303T5L, Light Sources) as the UV light source, which was similar to that reported by Li et al. [2]. The photon flux (I_0) from the UV source to the solution, the average fluence rate (I_s) and the effective path length (L) were $(4.15 \pm 0.02) \times 10^{-6}$ einstein s^{-1}, 1.47×10^{-8} einstein s^{-1} cm^{-2} (6.94 mW cm^{-2}) and (3.54 ± 0.01) cm, respectively [34].

All photolysis experiments were conducted at (25 ± 0.5) °C, which was controlled by a thermostat (THD-2015, Tianheng, Ningbo, China). Solution pH (6.6–12.3) was buffered by phosphate (10 mM), borate (10 mM) and sodium hydroxide (10 mM), and the absorption of buffers at 253.7 nm was negligible. To minimize the interference of oxygen dissolved in the solution to photolysis experiments, oxygen was removed by nitrogen gas (N_2, ≥99.99%). Photolysis experiments were initiated by UV irradiation with the addition of p-BQ (40 μM, unless otherwise noted) and MCAA (40 μM, unless otherwise noted) into the buffered solutions, and samples were withdrawn at predetermined time intervals and analyzed (always within 24 h) without quenching of residual p-BQ in the samples for the negligible depletion of MCAA by p-BQ. All experiments were repeated at least three times independently, and average values with one standard deviation (±SD) were presented.

2.3. Analytical methods

A pH meter, namely UB-7, Denver Instrument, was used for the determination of solution pH. Anions (chloride anion and

monochloroacetate anion) were quantified by an ion chromatograph (Dionex ICS-3000) with 30 mM KOH as isocratic eluent at 1.0 mL min^{-1}, and the suppressor current was 75 mA. Dionex ICS-3000 was equipped with a Dionex AS19 column (4×250 mm) and a Dionex AG19 guard column (4×50 mm). The analysis of p-BQ was conducted by a Waters 1525 high performance liquid chromatography (HPLC) with a Waters 2487 dual λ detector and a Waters symmetry C18 column (150 mm $\times$ 4.6 mm, 5 μm). The eluent of 0.1% acetic acid and methanol [90:10 (v/v)] was set at a flow rate of 1.0 mL min^{-1}.

2.4. Computation details

Density functional theory (DFT) [35–37] based calculations were carried out to investigate the homogeneous gas-phase transformation of p-BQ without environmental effect, which could help to confirm the generation of e$_{aq}^-$ from the photolysis of p-BQ under UV irradiation at 253.7 nm. The geometrical parameters of the structures in the gas phase were optimized through DFT [35–37] (the ground states, the first triplet states and the transition states) and time-dependent density-functional theory (TDDFT) [38] (the first excited singlet states) based on method B3LYP [39,40] with 6-311++G (3df,3pd) [41–43] basis set as implemented in the Gaussian 09 package [44]. Vibrational frequencies of the structures were also calculated at the same level. The optimized structures of reactants, intermediates, transition states and products are displayed in Fig. S1. The structures of the cage clusters of water $(H_2O)_6$ and $(H_2O)_6^-$ were optimized at the B3LYP/6-311++G (3df,3pd) level of theory for e$_{aq}^-$, and the energy of e$_{aq}^-$ was obtained by the method proposed by Zakharov et al. [45]. The detailed optimized structures of $(H_2O)_6$ and $(H_2O)_6^-$ were shown in the previous research [34], and the relative enthalpy of e$_{aq}^-$ was calculated to be -2.6 kcal mol^{-1} [34]. The properties of structures are provided in the Supplementary Data (Text S1 and Table S1).

3. Results and discussion

3.1. Mechanism of the photolysis of p-BQ under UV irradiation at 253.7 nm

3.1.1. Confirmation of the direct triplet mechanism for the formation of p-hydroquinone in the p-BQ/UV process

The photolysis of p-BQ (**A**) could induce the formation of p-HOC$_6$H$_4$OH (**G**) under UV irradiation at 253.7 nm via the direct triplet mechanism [26]. The pathways for the transformation of p-BQ were proposed in Scheme 1a. As shown in Scheme 1a, the first excited singlet state of p-BQ (**B**) was firstly yielded (53.0 kcal mol^{-1}), and the first triplet state of p-BQ (**C**) (the major species) was then yielded by intersystem crossing of **B** (-2.4 kcal mol^{-1}) [26,28–33]. With the quenching of **C** back to **A** as a competing pathway (-50.6 kcal mol^{-1}), the reduction of **C** by water molecule then led to the formation of 4,6-dihydroxycyclohexa-2,4-dienone (**D**) (-46.1 kcal mol^{-1}) [26]. In detail, the nucleophilic addition of OH$^-$ occurred at the α–β conjugated system of p-BQ (from **C$_1$** to **C$_2$**), followed by the protonation to induce the formation of **D** [46], which is 1,4-addition reaction [46,47]. With proton or hydroxyl ion as the catalyst, **D** could rearrange to hydroxy-p-hydroquinone (**E**) (-23.0 kcal mol^{-1}) [26], which could induce the reduction of **A** to **G** with the release of hydroxy-p-benzoquinone (**F**) (-6.7 kcal mol^{-1}) [26].

As the dominant step in the direct triplet mechanism (Scheme 1a) [26], the transformation of **C** to **D** was much more thermodynamically feasible than those in the OH$^\bullet$ (Scheme 1b) and electron transfer [Reaction (S2)] mechanisms, both of which were endothermic (6.2 kcal mol^{-1} for the OH$^\bullet$ mecha-
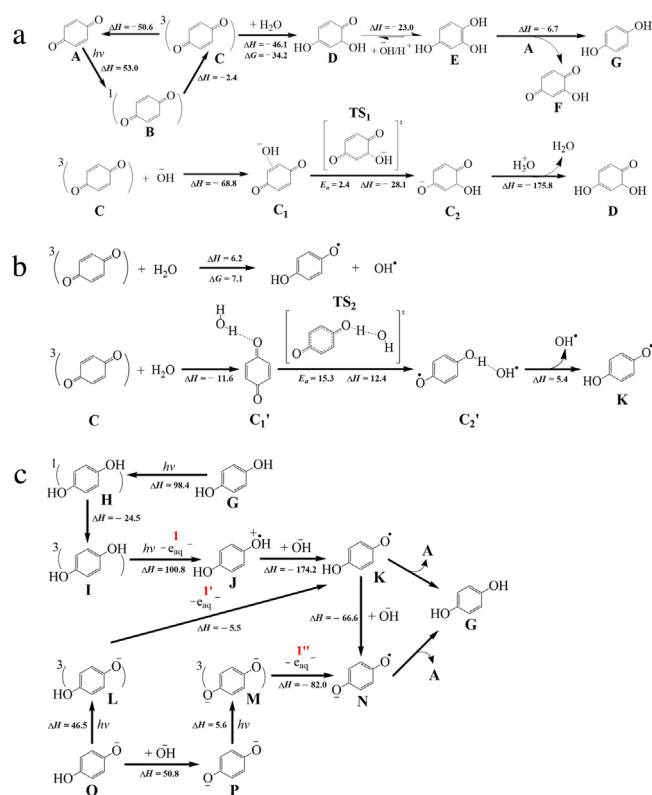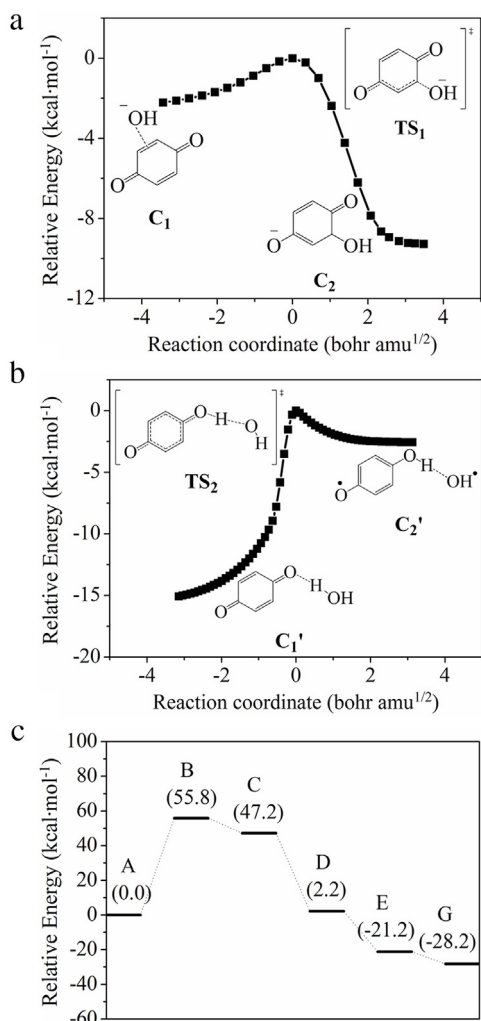

Scheme 1. Proposed pathways for the transformation of p-BQ under UV irradiation at 253.7 nm. (a) The formation of p-hydroquinone from p-BQ with water molecule via the direct triplet mechanism. (b) The OH$^\bullet$ mechanism. (c) The transformation of p-hydroquinone under UV irradiation at 253.7 nm. The energies (relative enthalpies and free energies) reported herein were calculated with zero-point energy (ZPE) correction and given in kcal mol^{-1}.

nism and 124.3 kcal mol^{-1} for the electron transfer mechanism). The energy barrier of the reaction **C** + OH$^-$ → **D** was calculated to be 2.4 kcal mol^{-1} with **TS$_1$** as the transition state (Fig. 1a and Scheme 1a). The predicted vibrational frequencies of **TS$_1$** (364.98i cm^{-1}) and intrinsic reaction coordinate (IRC) calculation shows that **TS$_1$** connected **C$_1$** and **C$_2$** (Fig. 1a). Kinetically, the energy barrier in Scheme 1a was much lower than those in Scheme 1b (15.3 kcal mol^{-1}) and Reaction (S2) (larger than 124.3 kcal mol^{-1}). The rate-determining step in the OH$^\bullet$ mechanism was **C$_1$'** → **C$_2$'** with **TS$_2$** as the transition state (Fig. 1b and Scheme 1b). IRC calculation shows that **TS$_2$** (1463.72i cm^{-1}) connected **C$_1$'** and **C$_2$'** (Fig. 1b). Obviously, the formation of p-hydroquinone via the direct triplet mechanism [26] was confirmed by the difference of the energy barriers in the three reaction paths.

According to the energy profile of minimum energy path (MEP) from **A** to **G** (Fig. 1c), **A** was thermodynamically feasible to induce the formation of **G**. The photolysis of **G** at 253.7 nm could induce **G** back to **A** [27] with a pathway displayed in Scheme 1c.

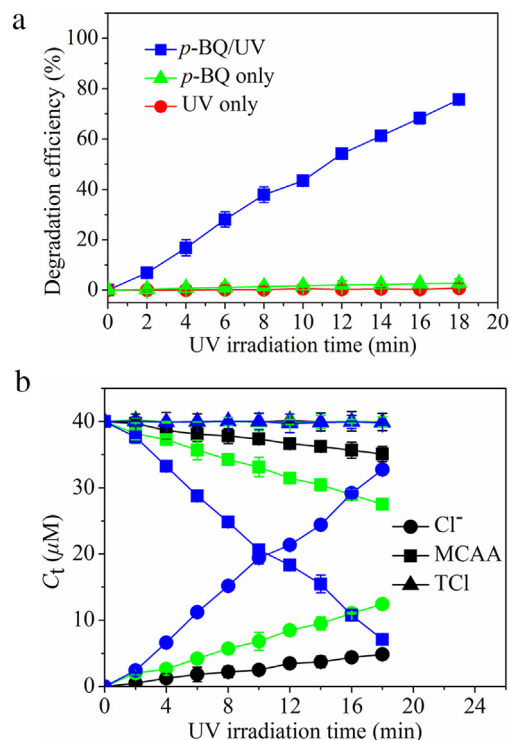#### 3.1.2. Mechanism of the generation of e$_{aq}^-$ from p-hydroquinone in the p-BQ/UV process

The photoionization of phenols and their anions in water are biphotonic [48] and monophotonic [48], respectively. Both the first excited singlet states and the first triplet states are the intermediates of phenols [49], and only those first triplet states are the intermediate electronic states of their anions [49]. Moreover, the phenoxyl radicals and e$_{aq}^-$ are directly generated from the first triplet states [48,49]. p-Hydroquinone has three dominant forms: p-HOC$_6$H$_4$OH (**G**), p-HOC$_6$H$_4$O$^-$ (**O**) and p-$^-$OC$_6$H$_4$O$^-$ (**P**) with p$K_{a1} = 9.85$, and p$K_{a2} = 11.4$ [50] (Text S2 and Fig. S2). As shown

Fig. 1. (a) Minimum energy path (MEP) of reaction from C_1 to C_2 calculated at the B3LYP/6-311++G (3df,3pd) level of theory. (b) MEP of reaction from C_1' to C_2'. (c) Energy profile of MEP for the transformation pathway involved in Scheme 1a.

Fig. 2. (a) Degradation efficiency of MCAA ($40\,\mu M$) in the p-BQ/UV process at pH 12.0. (b) Total mass balances of chlorine (TCl) during the MCAA ($40\,\mu M$) degradation in the p-BQ/UV process at different pH [6.6 (black), 9.2 (green), 12.0 (blue)]. Total chlorine (TCl) was calculated by the equation of TCl = [MCAA] + [Cl$^-$], and the concentration of species was molar concentration. Error bars represent the standard deviation from triplicate experiments. (For interpretation of the references to color in this figure legend, the reader is referred to the web version of this article.)

in Scheme 1c, **G** could release e_{aq}^- and p-benzosemiquinone radical (**K**) by photon absorption and deprotonation [49], where the first excited singlet state of p-hydroquinone (**H**), the first triplet state of p-hydroquinone (**I**) and protonated p-benzosemiquinone radical (**J**) as three intermediates were involved [49]. The generation of e_{aq}^- from **G** was biphotonic [48] with **G** and **I** as the photon acceptors [49], and **I** was formed from **H** through intersystem crossing [28,29,49]. The newly isolated e_{aq}^- from **G** could be quenched by proton to H$^\bullet$ rapidly ($2.3 \times 10^{10}\,M^{-1}\,s^{-1}$) [12], and the proton was generated from **J** with pK_a(**J**) = -1.1 [50]. The generation of e_{aq}^- from p-hydroquinone anion (**O**) and p-hydroquinone dianion (**P**) was monophotonic with the photon accepted by **O** and **P** [48], where the first triplet state of p-hydroquinone anion (**L**) and the first triplet state of p-hydroquinone dianion (**M**) were the intermediates [48]. **O** and **P** could release **K** and p-benzosemiquinone radical anion (**N**) with the generation of e_{aq}^- [27]. The newly generated **K** and **N** could be converted back to **G** with the release of **A** ($8 \times 10^7\,M^{-1}\,s^{-1}$) [51]. Kinetically, the energy barriers of the generation of e_{aq}^- from p-HOC$_6$H$_4$OH (**G**), p-HOC$_6$H$_4$O$^-$ (**O**) and p-$^-$OC$_6$H$_4$O$^-$ (**P**) were $100.8\,kcal\,mol^{-1}$, $46.5\,kcal\,mol^{-1}$ and $5.6\,kcal\,mol^{-1}$, respectively.

Consequently, the UV photolysis of p-BQ in aqueous solution via the direct triplet mechanism was theoretically confirmed by the thermodynamical and kinetic preference for the transformation from **C** to **D** in Scheme 1a. As an initiator [26], p-BQ (**A**) could induce the formation of p-HOC$_6$H$_4$OH (**G**) with water molecule as the original reductant (hydrogen donor). The generation of e_{aq}^- from **O** and **P** was much more efficient than that from **G**. Furthermore, one mole of **G**, **O** or **P** could theoretically generate two moles of e_{aq}^- with **G**, **O** or **P** back to **A**.

3.2. The generation of e_{aq}^- in the p-BQ/UV process

In order to validate the theoretical prediction, MCAA (the probe of e_{aq}^-) [12] was used to detect e_{aq}^- generated during the UV photolysis of p-BQ in aqueous solution. The degradation of MCAA could be achieved in the p-BQ/UV process at pH 12.0 (Fig. 2a), where p-HOC$_6$H$_4$O$^-$ and p-$^-$OC$_6$H$_4$O$^-$ are the two dominant forms of p-hydroquinone (Text S2 and Fig. S2). Moreover, the deoxygenated solution should be guaranteed to minimize the interference of oxygen to the degradation efficiency for the efficient quenching of e_{aq}^- by the oxygen dissolved in the solution ($1.9 \times 10^{10}\,M^{-1}\,s^{-1}$) [12]. The UV absorption of MCAA at 253.7 nm was so weak [52] that the direct photolysis of MCAA was undoubtedly less than 1% within 18 min. In contrast, a higher degradation efficiency of MCAA (76%) with a pseudo-zero-order rate constant (k, $\mu M\,min^{-1}$) of (1.72 ± 0.04) $\mu M\,min^{-1}$ was observed within 18 min in the presence of p-BQ. In addition, control experiment shows that less than 3% of MCAA was directly degraded by p-BQ within 24 h in the dark. These results indicate that the degradation of MCAA was induced by some reactive species produced during the UV photolysis of p-BQ in aqueous solution.

To verify the dominant reactive species responsible for the degradation, the mass balances during the kinetic runs were evaluated at different pH (Fig. 2b). The total chlorine (TCl) was calculated by the equation of TCl = [MCAA] + [Cl$^-$], with the molar concentra-

Table 1
Rate constants (k) of MCAA (40 μM) degradation and chloride ion formation in the p-BQ/UV process.

pH	Species	k (μM min^{-1})	R^2
6.6	MCAA	-0.2709 ± 0.0092	0.9897
	Cl$^-$	0.2677 ± 0.0076	0.9929
9.2	MCAA	-0.6819 ± 0.0093	0.9983
	Cl$^-$	0.6779 ± 0.0123	0.9970
12.0	MCAA	-1.8441 ± 0.0413	0.9955
	Cl$^-$	1.8351 ± 0.0437	0.9949

tion as the concentration of species. As shown in Table 1, the rate constants of chloride ion formation were comparable to those of MCAA degradation at different pH, respectively. Moreover, the total chlorine (TCl) was almost constant (Fig. 2b). The mass balances indicate that the chlorine in MCAA was released as Cl$^-$ (more than 98%), which was a reductive process.

The UV photolysis of p-BQ in aqueous solution can produce some reactive species, e.g., e_{aq}^-, semiquinone radical and H$^{\bullet}$ (quenching of e_{aq}^- by H$^+$ in acidic solution) [12], as reported in previous studies [26,27]. H$^{\bullet}$ (-2.3 V) [12] and e_{aq}^- (-2.9 V) [12] are much more reductive than semiquinone radical, which has a standard reduction potential of larger than 0.0 V [53], and it is obvious that the degradation of MCAA was caused by e_{aq}^- and/or H$^{\bullet}$. However, the degradation of MCAA by H$^{\bullet}$ induces the release of H$_2$ by abstracting H rather than the dechlorination of MCAA with Cl$^-$ release [12]. Consequently, with e_{aq}^- as the dominant reactive species, the degradation of MCAA could be efficiently induced by the UV photolysis of p-BQ at pH 12.0, and Cl$^-$ was the sole chlorine-bearing degradation product. The observed dechlorination of MCAA confirmed the generation of e_{aq}^- in the p-BQ/UV process at pH 12.0, as well as the rationality of the pathways proposed in Scheme 1a and c (the generation of e_{aq}^- from p-HOC$_6$H$_4$O$^-$ and p-$^-$OC$_6$H$_4$O$^-$). The formation of p-hydroquinone by the UV photolysis of p-BQ in aqueous solution was via the direct triplet mechanism, which could also be verified by the observed dechlorination of MCAA. Unfortunately, the experimental confirmation of the e_{aq}^- generation from the UV photolysis of the standard p-hydroquinone is difficult to carry out, since p-hydroquinone is so unstable that its stock solution is hard to prepare without addition of antioxidants [54].

3.3. Influence of variables on the generation of e_{aq}^- in the p-BQ/UV process

3.3.1. p-BQ

As shown in Scheme 1, p-BQ is theoretically critical for the generation of e_{aq}^-. As an initiator [26] and photosensitizer [27] in the process, the influence of p-BQ concentration (0–60 μM) on the generation of e_{aq}^- was investigated at pH 12.0. The results show that the degradation efficiency of MCAA was dependent on the p-BQ concentration with a maximum efficiency obtained at 35 μM, as shown in Fig. 3a. Furthermore, a positive linear correlation between k and the p-BQ concentration with $k/[p\text{-BQ}]_0 = (63.3 \pm 6.1)\,\text{min}^{-1}$ was observed in Fig. 3b when the p-BQ concentration was below 35 μM. The positive linear correlation indicates that more p-BQ could induce more extent of e_{aq}^- generation for the MCAA degradation, and the rate of e_{aq}^- generation was determined to be about $(63.3 \pm 6.1)\,\mu\text{M min}^{-1}$ per mM p-BQ herein. When the concentration was above 35 μM, the quenching of e_{aq}^- by p-BQ ($1.25 \times 10^9\,\text{M}^{-1}\,\text{s}^{-1}$) [55] is more significant than that by MCAA ($1.0 \times 10^9\,\text{M}^{-1}\,\text{s}^{-1}$) [12], which might be the cause for the deceleration in Fig. 3b.
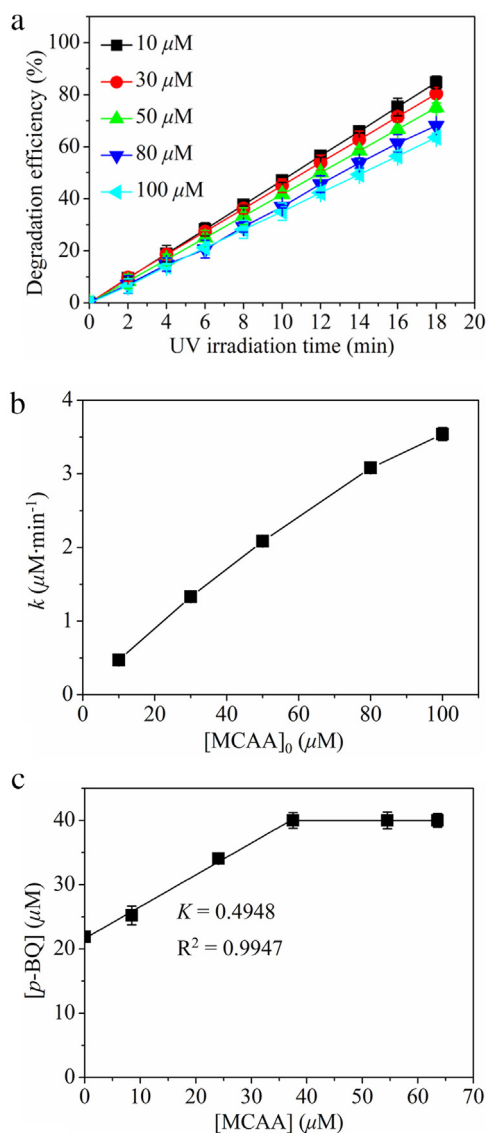
3.3.2. Monochloroacetic acid (MCAA)

MCAA acts as an electron acceptor in the p-BQ/UV process, and there are other competitors for the quenching of e_{aq}^- to induce
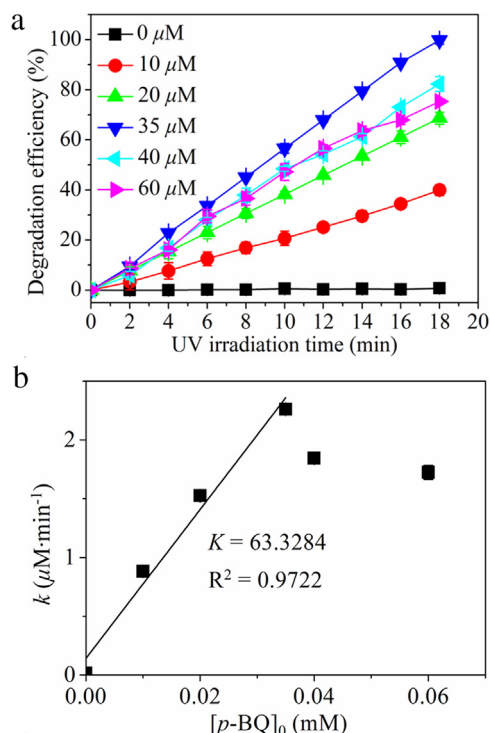
Fig. 3. (a) Effect of p-BQ concentration (0–60 μM) on the degradation efficiency of MCAA (40 μM) in the p-BQ/UV process at pH 12.0. (b) The correlation between the degradation rate constants (k) and the p-BQ concentration (0–60 μM) at pH 12.0. The solid line indicates the best linear fit (b).

the competing reactions. With the concentration from 10 μM to 100 μM, the influence of the MCAA concentration on the degradation efficiency was investigated in the p-BQ/UV process at pH 12.0 (Fig. 4a). The similar dependence on the MCAA concentration [34] was observed, as shown in Fig. 4b. The reason for the dependence herein might be similar to that in the phenol/UV process reported in the previous study [34]. Since p-BQ is even much more sensitive than phenol for UV absorption at 253.7 nm [27], the increase of MCAA concentration may only affect the proportion of the involved competing reactions of e_{aq}^- [56] rather than the UV absorption for the generation of e_{aq}^- from p-BQ in the process. Moreover, the correlation between the amounts of p-BQ and MCAA degraded in the p-BQ/UV process was shown in Fig. 4c, and a linear correlation with the slope of 0.495 (± 0.021) was observed when the amount of MCAA degraded was less than 40 μM.

During the UV photolysis of p-BQ, with the hydrogen donation of water molecule, one mole of p-BQ can generate one mole of hydroxy-p-hydroquinone, which can induce the transformation of p-BQ to p-hydroquinone with a mole ratio of 1:1, as reported in the previous study [26]. Thus, the mole ratio of the transformed p-BQ to the generated p-hydroquinone is 2:1, as shown in Scheme 1a. The generated p-hydroquinone can generate e_{aq}^- with a molar ratio of 1:2, and p-hydroquinone is transformed to p-BQ with a molar ratio of 1:1 [27], as shown in Scheme 1c. Theoretically, the mole ratio of the transformed p-BQ to the generated e_{aq}^- is 1:2, which was consistent with the result in Fig. 4c. The slope in Fig. 4c indicates that the degradation (transformation) of one mole of p-BQ could induce the degradation of about two moles of MCAA under UV irradiation, which implies that the mole ratio of the degraded (transformed) p-BQ to the generated e_{aq}^- was 1:2 in the p-BQ/UV process at pH 12.0. Thus, with water molecule as the original source of e_{aq}^-, the hydrogen donation of water molecule in the process was also confirmed. Moreover, less than 50% of 40 μM p-BQ (Fig. 4c) was involved in the generation of e_{aq}^- for the degradation of MCAA, which indicates

Fig. 5. (a) Effect of pH (6.6–12.3) on the degradation efficiency of MCAA (40 μM) in the *p*-BQ/UV process. (b) The degradation rate constants (*k*) versus pH, and the solid line is the pH-dependent molar ratio of the anions (the integration of *p*-HOC$_6$H$_4$O$^-$ and *p*-$^-$OC$_6$H$_4$O$^-$).
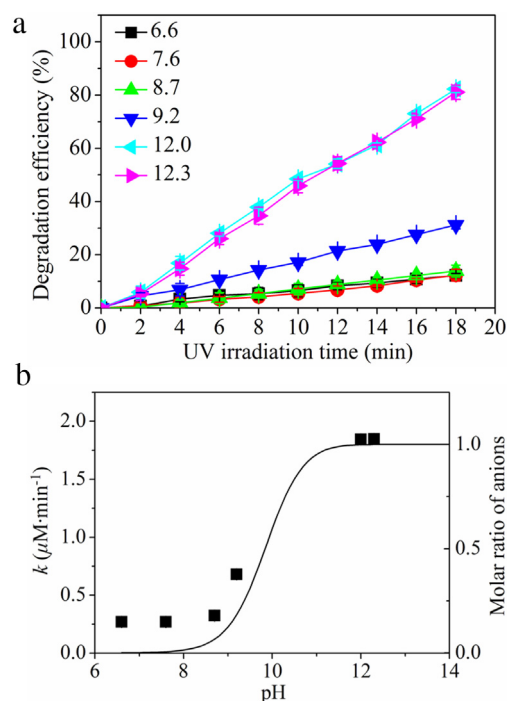
Fig. 4. (a) Effect of MCAA concentration (10–100 μM) on the degradation efficiency of MCAA in the *p*-BQ/UV process at pH 12.0. (b) The correlation between the degradation rate constants (*k*) and the MCAA concentration (10–100 μM) at pH 12.0. (c) The linear relationship between the amounts of *p*-BQ and MCAA degraded. The solid line indicates the best linear fit (c).

that the competing reactions of *p*-BQ in the process are significant. The derivatives of *p*-BQ could also induce the generation of e$_{aq}^-$ under UV irradiation in aqueous solution, as shown in Fig. 4c.

3.3.3. pH

According to Scheme 1a, the transformation of *p*-BQ to hydroxy-*p*-hydroquinone by water molecule and the reduction of *p*-BQ to *p*-hydroquinone by hydroxy-*p*-hydroquinone were much more feasible than the generation of e$_{aq}^-$ from *p*-hydroquinone in Scheme 1c, which indicates that the steps for the transformation of *p*-BQ to *p*-hydroquinone were not the rate-determining ones for the generation of e$_{aq}^-$ in the process. Thus, it could be thought that the solution pH might not have a significant influence on the transformation of *p*-BQ to *p*-hydroquinone with hydroxy-*p*-hydroquinone as the intermediate and reductant, even though the solution pH can govern the forms of hydroxy-*p*-hydroquinone (molecule or anions), which could induce the exothermic or slightly endothermic reduction of *p*-BQ to *p*-hydroquinone [Reactions (S3–S5)].

As the direct source of e$_{aq}^-$ in the *p*-BQ/UV process [26,27], the forms of *p*-hydroquinone are determined by the solution pH (Text S2 and Fig. S2), and the anions (*p*-HOC$_6$H$_4$O$^-$ and *p*-$^-$OC$_6$H$_4$O$^-$) may play a key role on the generation of e$_{aq}^-$. Kinetically, the energy barriers of the generation of e$_{aq}^-$ from *p*-HOC$_6$H$_4$O$^-$ and *p*-$^-$OC$_6$H$_4$O$^-$ were 46.5 kcal mol^{-1} and 5.6 kcal mol^{-1}, respectively, which were much lower than that from *p*-HOC$_6$H$_4$OH (100.8 kcal mol^{-1}), according to Scheme 1c. Obviously, the difference of the energy barriers indicates that higher pH would promote the generation of e$_{aq}^-$ from *p*-hydroquinone, which is verified by Fig. 5a and b. Fig. 5a shows the influence of pH on the degradation efficiency of MCAA with pH from 6.6 to 12.3. The degradation efficiency did not change from 6.6 to 8.7, followed by an obvious acceleration from 8.7 to 12.0, and the maximum degradation efficiency was likely observed at pH 12.3. Moreover, the tendency was corroborated by the dependence of *k* on pH (Fig. 5b), which was supported by the molar ratio of the anions (the integration of *p*-HOC$_6$H$_4$O$^-$ and *p*-$^-$OC$_6$H$_4$O$^-$) versus pH except for *k* at pH below 8.7. The existence of the molecular *p*-hydroquinone (*p*-HOC$_6$H$_4$OH) might be responsible for the exception.

According to Fig. 2b and Table 1, e$_{aq}^-$ was indeed generated in the *p*-BQ/UV process even at pH 6.6, being the dominant reactive species. However, UV irradiation at 253.7 nm (112.7 kcal mol^{-1}) cannot accomplish the generation of e$_{aq}^-$ from *p*-HOC$_6$H$_4$OH efficiently, since its energy barrier was 100.8 kcal mol^{-1}. Fortunately, the decline of the energy barrier could be induced via a MS-EPT pathway [57] involved in the *p*-BQ/UV process. With phosphate ion or hydroxyl ion as the proton-acceptor bases, *p*-HOC$_6$H$_4$OH can release electron to the electron-acceptor (MCAA) via MS-EPT pathway without H$^\bullet$ formation [57] in the *p*-BQ/UV process. The basicity of the proton–acceptor base is the primary factor for the MS-EPT pathway [57], and hydroxyl ion is acceptable to be selected as the proton–acceptor base, since hydroxyl ion (OH$^-$, pK_b = −1.7) [57] is much more basic than phosphate ion (HPO$_4^{2-}$, pK_b = 6.8) [57].
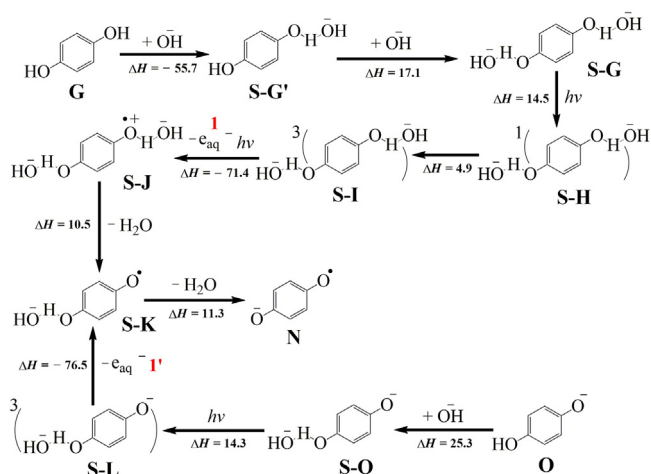
Scheme 2. The transformation of p-hydroquinone involving MS-EPT pathway under UV irradiation at 253.7 nm. The energies (relative enthalpies) reported herein were calculated with ZPE correction and given in kcal mol^{-1}.

3.4. MS-EPT pathway involved in the p-BQ/UV process

With hydroxyl ion as proton-acceptor base, the pathway of the generation of e$_{aq}^-$ via MS-EPT pathway was proposed and displayed in Scheme 2. As shown in Scheme 2, **G** was stabilized by hydroxyl ion via the H-bond between the hydrogen of the hydroxyl of **G** and the oxygen of hydroxyl ion with two consecutive steps, which were exothermic by 55.7 kcal mol^{-1} and endothermic by 17.1 kcal mol^{-1}, respectively. The generation of e$_{aq}^-$ from the stabilized p-hydroquinone (**S-G**) was via a biphotonic pathway with the first excited singlet state (**S-H**), the first triplet state (**S-I**) and dihydrated p-benzosemiquinone radical anion (**S-J**) as the intermediates, and the pathway was similar to that of the generation of e$_{aq}^-$ from **G** in Scheme 1c. **O** was stabilized by hydroxyl ion to the stabilized p-hydroquinone anion (**S-O**), which was endothermic by 25.3 kcal mol^{-1}. Similarly, **S-O** could release e$_{aq}^-$ via a monophotonic pathway, and the first triplet state (**S-L**) was the intermediate. Kinetically, the addition of hydroxyl ion indeed facilitated the generation of e$_{aq}^-$ from **S-G** and **S-O** with much lower energy barriers (14.5 kcal mol^{-1} and 14.3 kcal mol^{-1}, respectively).

The involvement of proton-acceptor base (hydroxyl ion) in the process thermodynamically facilitated the generation of e$_{aq}^-$ from p-hydroquinone without formation of high-energy intermediate via MS-EPT pathway (Scheme 2) [57]. The crucial factor in the acceleration was the H-bond involved in the process [57]. With the H-bond involved in the process, the property of p-hydroquinone has been altered (Text S1 and Fig. S1). With the generation of e$_{aq}^-$ from **S-G**, the proton was accepted by hydroxyl ion in **S-G**, which could be observed by the change of the bond lengths of the H-bond [from 1.049 Å (**S-G**) to 0.990 Å (**S-J**)] and the hydroxyl [from 1.502 Å (**S-G**) to 1.737 Å (**S-J**)] (Fig. S1). The occurrence of electron-proton transfer from **S-G** to different acceptors (MCAA and hydroxyl ion) could take place simultaneously without formation of H• [57]. According to Scheme 2 and Fig. S1, simultaneous electron-proton transfer occurred from **S-O** to different acceptors (MCAA and hydroxyl ion) via similar pathway. As the crucial factor, the H-bond involved in the process made the properties of the undissociated p-hydroquinones (RC$_6$H$_4$OH, R = OH or O$^-$) similar to those of their conjugate bases (Text S1), and the H-bond could also stabilize the intermediates (e.g., **J** and **K**) (Table S1).
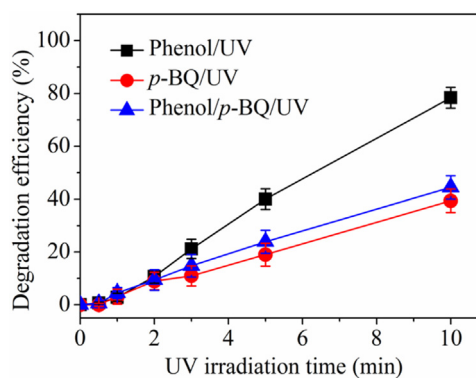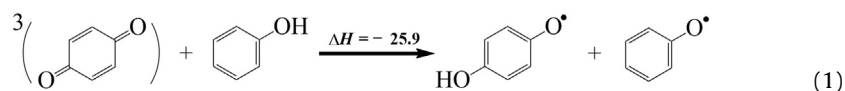

Fig. 6. Degradation efficiency of MCAA (80 μM) with the addition of 40 μM phenol and 40 μM p-BQ in the solution at pH 12.0.

Consequently, with MS-EPT pathway involved in the process, the undissociated p-hydroquinones were stabilized by hydroxyl ion with the H-bond. The generation of e$_{aq}^-$ from the undissociated p-hydroquinones with the stabilization was much more efficient, which could explain the phenomena at pH below 8.7. Eventually, the coincidence in Fig. 5b indirectly indicates the formation of p-hydroquinone.
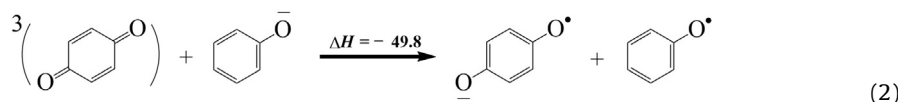
3.5. Addition of phenol in the p-BQ/UV process

The e$_{aq}^-$ generation was detected in the phenol/UV process [34] and the p-BQ/UV process. The triplet state of p-BQ can be quenched by phenol with the formation of p-benzosemiquinone radical and phenoxyl radical [58,59], which is much more thermodynamically feasible [Reactions (1)–(2)] than the e$_{aq}^-$ generation from the UV photolysis of phenol with the formation of phenoxyl radical [34]. In addition, the enthalpies of phenol and phenolate were cited from the previous research [34]. It is reasonable to expect the enhancement of the e$_{aq}^-$ generation from the UV photolysis of p-BQ with the addition of phenol. Actually, the presence of phenol in the p-BQ/UV process induced the subtle enhancement, as shown in Fig. 6. The e$_{aq}^-$ generation from p-BQ and phenol is illustrated in Fig. 6 with the addition of 40 μM phenol, 40 μM p-BQ and 80 μM MCAA in the solution at pH 12.0, respectively. The molar absorption coefficient of p-BQ is 19000 M^{-1} cm^{-1} at 253.7 nm [27], which indicates that p-BQ is much more photosensitive than phenol (520 M^{-1} cm^{-1} for C$_6$H$_5$OH [27] and 942.43 M^{-1} cm^{-1} for C$_6$H$_5$O$^-$ [34] at 253.7 nm). Thus, p-BQ might be the primary photosensitizer in the phenol/p-BQ/UV process, which makes it possible for the triplet state of p-BQ to be quenched by phenol [58,59]. Moreover, the e$_{aq}^-$ generation from the UV photolysis of phenol (40 μM) at pH 12.0 might be inhibited by the presence of p-BQ (40 μM) in the phenol/p-BQ/UV process, which could be confirmed by the subtle enhancement in the p-BQ/UV process with the addition of phenol (Fig. 6). The subtle enhancement in Fig. 6 might be induced by the electron donation of phenolate in the process.

The influence of phenol on the degradation efficiency with p-BQ is complex, and it is difficult to assess the respective contribution of the UV photolysis of phenol, the UV photolysis of p-BQ, and the hydrogen/electron donation of phenol to the e$_{aq}^-$ generation in the phenol/p-BQ/UV process, since the quantum yield of e$_{aq}^-$ in the p-BQ/UV process is difficult to obtain.

$$\left(\begin{array}{c} ^3 \end{array} \right) + \text{PhOH} \xrightarrow{\Delta H = -25.9} \text{products} \tag{1}$$

$$3\left(\begin{array}{c}\text{O}\\ \hline \\ \text{O}\end{array}\right) + \begin{array}{c}\overline{\text{O}}\\ \hline \end{array} \xrightarrow{\Delta H = -49.8} \begin{array}{c}\text{O}^\bullet\\ \hline \\ \overline{\text{O}}\end{array} + \begin{array}{c}\text{O}^\bullet\\ \hline \end{array} \qquad (2)$$

4. Conclusions

The combination of *p*-BQ and UV irradiation (253.7 nm) to generate e_{aq}^- was demonstrated in the present work. The formation of *p*-hydroquinone by the UV photolysis of *p*-BQ in aqueous solution via the direct triplet mechanism was confirmed with DFT calculations. The pathway for the generation of e_{aq}^- from *p*-hydroquinone was further illuminated to obtain the energy barrier to interpret the enhancement of the e_{aq}^- generation at high pH. Both DFT calculations and experiment confirmed the crucial role of *p*-BQ, the hydrogen donation of water molecule and the formation of *p*-hydroquinone in the *p*-BQ/UV process. Furthermore, e_{aq}^- generated in the *p*-BQ/UV process was also available for the dechlorination of MCAA with the presence of some e_{aq}^- quenchers (e.g., dissolved oxygen, NO_2^- and NO_3^-) (Fig. S3).

The dependence of the efficiency on pH indicated that it may be favorable to apply the *p*-BQ/UV process in practice at strong alkaline conditions. When the practical wastewater is not at strong alkaline conditions, it can be treated by the UV photolysis of some quinones, which can induce the formation of much more acidic hydroquinones (pK_a is much less than 9.85). The *p*-BQ/UV process may provide an alternative for the establishment of e_{aq}^- based reduction processes by the photolysis of quinones, which are widely distributed in the environment [20]. The present work helps to understand the mechanism of e_{aq}^- generation from natural organic matters (NOM) [60], which usually contain quinone-like groups [61,62]. More detailed studies deserve to be conducted to investigate the effect of the coexistence of *p*-BQ and phenol on the e_{aq}^- generation in the process.

Acknowledgements

Appendix A. Supplementary data

Supplementary data associated with this article can be found, in the online version, at http://dx.doi.org/10.1016/j.apcatb.2017.03.081.

References

[1] B.P. Vellanki, B. Batchelor, A. Abdel-Wahab, Environ. Eng. Sci. 30 (5) (2013) 264–271.
[2] X. Li, J. Ma, G. Liu, J. Fang, S. Yue, Y. Guan, L. Chen, X. Liu, Environ. Sci. Technol. 46 (13) (2012) 7342–7349.
[3] X. Liu, S. Yoon, B. Batchelor, A. Abdel-Wahab, Sci. Total Environ. 454–455 (2013) 578–583.
[4] X. Liu, S. Yoon, B. Batchelor, A. Abdel-Wahab, Chem. Eng. J. 215–216 (2013) 868–875.
[5] X. Liu, B.P. Vellanki, B. Batchelor, A. Abdel-Wahab, Chem. Eng. J. 237 (2014) 300–307.
[6] B. Jung, R. Nicola, B. Batchelor, A. Abdel-Wahab, Chemosphere 117 (2014) 663–672.
[7] Z. Song, H. Tang, N. Wang, L. Zhu, J. Hazard. Mater. 262 (2013) 332–338.
[8] Y. Qu, C. Zhang, F. Li, J. Chen, Q. Zhou, Water Res. 44 (9) (2010) 2939–2947.
[9] Y. Qu, C.-J. Zhang, P. Chen, Q. Zhou, W.-X. Zhang, Chemosphere 107 (2014) 218–223.
[10] Y. Wang, P. Zhang, J. Environ. Sci. 26 (11) (2014) 2207–2214.
[11] C. Zhang, Y. Qu, X. Zhao, Q. Zhou, Clean–Soil Air Water 43 (2) (2015) 223–228.
[12] G.V. Buxton, C.L. Greenstock, W.P. Helman, A.B. Ross, J. Phys. Chem. Ref. Data 17 (2) (1988) 513–886.
[13] A. Kumar, J.A. Walker, D.M. Bartels, M.D. Sevilla, J. Phys. Chem. A 119 (34) (2015) 9148–9159.
[14] D.H. Paik, I.-R. Lee, D.-S. Yang, J.S. Baskin, A.H. Zewail, Science 306 (5696) (2004) 672–675.
[15] A.E. Bragg, J.R.R. Verlet, A. Kammrath, O. Cheshnovsky, D.M. Neumark, J. Am. Chem. Soc. 127 (43) (2005) 15283–15295.
[16] B.P. Vellanki, B. Batchelor, J. Hazard. Mater. 262 (2013) 348–356.
[17] W.W. Mohn, J.M. Tiedje, Microb. Rev. 56 (3) (1992) 482–507.
[18] P. Calza, E. Pelizzetti, J. Photochem. Photobiol. A: Chem. 162 (2–3) (2004) 609–613.
[19] H. Park, C.D. Vecitis, J. Cheng, N.F. Dalleska, B.T. Madere, M.R. Hoffmann, Photochem. Photobiol. Sci. 10 (12) (2011) 1945–1953.
[20] M. Aeschbacher, C. Graf, R.P. Schwarzenbach, M. Sander, Environ. Sci. Technol. 46 (9) (2012) 4916–4925.
[21] R.A. Doong, H.C. Chiang, Environ. Sci. Technol. 39 (19) (2005) 7460–7468.
[22] V. Gómez-Toribio, A.B. García-Martín, M.J. Martínez, Á.T. Martínez, F. Guillén, Appl. Environ. Microbiol. 75 (12) (2009) 3944–3953.
[23] R.A. Royer, W.D. Burgos, A.S. Fisher, R.F. Unz, B.A. Dempsey, Environ. Sci. Technol. 36 (9) (2002) 1939–1946.
[24] Y. Song, G.R. Buettner, Free Radic. Biol. Med. 49 (6) (2010) 919–962.
[25] F. Li, G. Li, B. Liu, X. Zhang, Desalin. Water Treat. 53 (7) (2015) 1933–1941.
[26] H. Görner, J. Phys. Chem. A 107 (51) (2003) 11587–11595.
[27] H.-I. Joschek, S.I. Miller, J. Am. Chem. Soc. 88 (14) (1966) 3273–3281.
[28] W. Wu, X. Wu, J. Zhao, M. Wu, J. Mater. Chem. C 3 (10) (2015) 2291–2301.
[29] X. Wu, W. Wu, X. Cui, J. Zhao, M. Wu, J. Mater. Chem. C 4 (14) (2016) 2843–2853.
[30] A.E. Alegría, A. Ferrer, E. Sepúlveda, Photochem. Photobiol. 66 (4) (1997) 436–442.
[31] A.I. Ononye, A.R. MacIntosh, J.R. Bolton, J. Phys. Chem. 90 (23) (1986) 6266–6270.
[32] A.I. Ononye, J.R. Bolton, J. Phys. Chem. 90 (23) (1986) 6270–6274.
[33] J. von Sonntag, E. Mvula, K. Hildenbrand, C. von Sonntag, Chem. Eur. J. 10 (2) (2004) 440–451.
[34] J. Gu, J. Ma, J. Jiang, L. Yang, J. Yang, J. Zhang, H. Chi, Y. Song, S. Sun, W.Q. Tian, Appl. Catal. B: Environ. 200 (2017) 585–593.
[35] P. Hohenberg, W. Kohn, Phys. Rev. 136 (3B) (1964) B864–B871.
[36] W. Kohn, L.J. Sham, Phys. Rev. 140 (4A) (1965) A1133–A1138.
[37] R.G. Parr, W. Yang, Oxford University Press, New York, 1989.
[38] R.E. Stratmann, G.E. Scuseria, M.J. Frisch, J. Chem. Phys. 109 (19) (1998) 8218–8224.
[39] C. Lee, W. Yang, R.G. Parr, Phys. Rev. B 37 (2) (1988) 785–789.
[40] A.D. Becke, J. Chem. Phys. 98 (7) (1993) 5648–5652.
[41] A.D. McLean, G.S. Chandler, J. Chem. Phys. 72 (10) (1980) 5639–5648.
[42] R. Krishnan, J.S. Binkley, R. Seeger, J.A. Pople, J. Chem. Phys. 72 (1) (1980) 650–654.
[43] M.J. Frisch, J.A. Pople, J.S. Binkley, J. Chem. Phys. 80 (7) (1984) 3265–3269.
[44] M.J. Frisch, G.W. Trucks, H.B. Schlegel, G.E. Scuseria, M.A. Robb, J.R. Cheeseman, G. Scalmani, V. Barone, B. Mennucci, G.A. Petersson, H. Nakatsuji, M. Caricato, X. Li, H.P. Hratchian, A.F. Izmaylov, J. Bloino, G. Zheng, J.L. Sonnenberg, M. Hada, M. Ehara, K. Toyota, R. Fukuda, J. Hasegawa, M. Ishida, T. Nakajima, Y. Honda, O. Kitao, H. Nakai, T. Vreven Jr., J.A. Montgomery, J.E. Peralta, F. Ogliaro, M. Bearpark, J.J. Heyd, E. Brothers, K.N. Kudin, V.N. Staroverov, R. Kobayashi, J. Normand, K. Raghavachari, A. Rendell, J.C. Burant, S.S. Iyengar, J. Tomasi, M. Cossi, N. Rega, J.M. Millam, M. Klene, J.E. Knox, J.B. Cross, V. Bakken, C. Adamo, J. Jaramillo, R. Gomperts, R.E. Stratmann, O. Yazyev, A.J. Austin, R. Cammi, C. Pomelli, J.W. Ochterski, R.L. Martin, K. Morokuma, V.G. Zakrzewski, G.A. Voth, P. Salvador, J.J. Dannenberg, S. Dapprich, A.D. Daniels, O. Farkas, J.B. Foresman, J.V. Ortiz, J. Cioslowski, D.J. Fox, *Gaussian* 09, in: Revision A. 02, Gaussian, Inc, Wallingford, CT, 2009.
[45] I.I. Zakharov, J. Struct. Chem. 55 (1) (2014) 1–7.
[46] M. Uchimiya, A.T. Stone, Chemosphere 77 (4) (2009) 451–458.
[47] J.A. Perlinger, V.M. Kalluri, R. Venkatapathy, W. Angst, Environ. Sci. Technol. 36 (12) (2002) 2663–2669.
[48] J. Feitelson, E. Hayon, A. Treinin, J. Am. Chem. Soc. 95 (4) (1973) 1025–1029.
[49] T. Alapi, A. Dombi, J. Photochem. Photobiol. A: Chem. 188 (2–3) (2007) 409–418.
[50] J.J. Warren, T.A. Tronic, J.M. Mayer, Chem. Rev. 110 (12) (2010) 6961–7001.
[51] V.A. Roginsky, L.M. Pisarenko, W. Bors, C. Michel, J. Chem. Soc. Perkin Trans. 2 (4) (1994) 871–876.
[52] C.H. Jo, A.M. Dietrich, J.M. Tanko, Water Res. 45 (8) (2011) 2507–2516.
[53] P. Wardman, J. Phys. Chem. Ref. Data 18 (4) (1989) 1637–1755.
[54] H.M. Torok, T. Jones, P. Rich, S. Smith, E. Tschen, Cutis 75 (1) (2005) 57–62.
[55] E.J. Hart, S. Gordon, J.K. Thomas, J. Phys. Chem. 68 (6) (1964) 1271–1274.

[56] W.M. Draper, D.G. Crosby, J. Agric. Food Chem. 31 (4) (1983) 734–737.
[57] D.R. Weinberg, C.J. Gagliardi, J.F. Hull, C.F. Murphy, C.A. Kent, B.C. Westlake, A. Paul, D.H. Ess, D.G. McCafferty, T.J. Meyer, Chem. Rev. 112 (7) (2012) 4016–4093.
[58] S. Canonica, B. Hellrung, J. Wirz, J. Phys. Chem. A 104 (6) (2000) 1226–1232.
[59] Y. Zhang, K.A. Simon, A.A. Andrew, R.D. Vecchio, N.V. Blough, Environ. Sci. Technol. 48 (21) (2014) 12679–12688.
[60] C.M. Sharpless, N.V. Blough, Environ. Sci.: Processes Impacts 16 (4) (2014) 654–671.
[61] M. Fujii, A. Imaoka, C. Yoshimura, T.D. Waite, Environ. Sci. Technol. 48 (8) (2014) 4414–4424.
[62] S. Kang, W. Choi, Environ. Sci. Technol. 43 (3) (2009) 878–883.